

## Differences in the neutralization of 2.4–10 keV $\text{Ne}^+$ scattered from the Cu and Au atoms of an alloy surface

T. M. Buck\*

*Department of Materials Science and Engineering, University of Pennsylvania, Philadelphia, Pennsylvania 19104-6272  
and Laboratory for Research on the Structure of Matter, University of Pennsylvania, Philadelphia,  
Pennsylvania 19104-6202  
and AT&T Bell Laboratories, Murray Hill, New Jersey 07974*

W. E. Wallace<sup>†</sup>

*Department of Materials Science and Engineering, University of Pennsylvania, Philadelphia, Pennsylvania 19104-6272  
and Laboratory for Research on the Structure of Matter, University of Pennsylvania, Philadelphia,  
Pennsylvania 19104-6202*

R. A. Baragiola

*Laboratory for Atomic and Surface Physics, Engineering Physics, University of Virginia, Charlottesville, Virginia 22901*

G. H. Wheatley\*

*AT&T Bell Laboratories, Murray Hill, New Jersey 07974*

J. B. Rothman

*Laboratory for Research on the Structure of Matter, University of Pennsylvania, Philadelphia,  
Pennsylvania 19104-6202*

R. J. Gorte

*Department of Chemical Engineering, University of Pennsylvania, Philadelphia, Pennsylvania 19104-6393  
and Laboratory for Research on the Structure of Matter, University of Pennsylvania, Philadelphia,  
Pennsylvania 19104-6202*

J. G. Tittensor

*Department of Chemical Engineering, University of Pennsylvania, Philadelphia, Pennsylvania 19104-6393  
(Received 2 November 1992)*

The neutralization behavior of low-energy  $\text{Ne}^+$  ions scattered from a compositionally ordered  $\text{Cu}_3\text{Au}(100)$  surface has been studied over a range of incident energy  $E_0$  from 2.4 to 10 keV. Ion fractions of Ne scattered from Cu atoms in the first, or first two, atom layers exhibited a sharp increase setting in at an  $E_0$  of 4–5 keV, reaching 70% at 10 keV for first-layer scattering. Inelastic energy losses, up to 130 eV, and Auger electron emission from Ne scattered from Cu, were also observed at incident energies above 4 keV. Ne scattered from the Au atoms on the same  $\text{Cu}_3\text{Au}(100)$  surface showed only the usual velocity-dependent Auger and resonance neutralization. An explanation of the Cu results is given in terms of Ne  $2s$  vacancy creation during the close collision of Ne, which is neutralized on the inward path, followed by autoionization on the outward path after scattering into the vacuum. Conversely, Ne cannot approach Au closely enough to form an appropriate inner-shell vacancy. This is due to the higher Coulombic repulsion created by the greater charge of the Au nucleus.

### I. INTRODUCTION

Since 1967, when D. Smith introduced ion scattering spectroscopy,<sup>1</sup> also known as low-energy ion scattering (LEIS), the problem of the neutralization of low-energy ions scattering from solid surfaces has been investigated experimentally and theoretically by many workers. This interest arose originally from a need to understand and correct for varying neutralization probabilities when performing quantitative composition and structure analysis of multicomponent surfaces using noble-gas ions with electrostatic energy analysis of the scattered particles.

These investigations have led to a complex picture of several mechanisms which may contribute to neutralization behavior in various situations,<sup>2–6</sup> and has been the subject of recent reviews.<sup>7</sup> In this paper we describe experiments on an alloy surface, over an energy range in which  $\text{Ne}^+$  ions scattered from one element, Au, are neutralized only by Auger and by resonance transitions involving electrons from an energy band in the solid as the ion approaches or leaves the surface. On the other hand, ions scattered from the other element, Cu, may pick up electrons in these same ways, but if neutralized on the incoming path, may be reionized by the close collision with

the Cu atom when the incident energy exceeds about 4 keV. Evidence of this process is seen in a pronounced increase in the ion fraction of the Ne scattered from Cu, shifts to lower energy in the LEIS Cu scattering peaks, and emission of Auger electrons from Ne scattered from Cu.

## II. EXPERIMENTAL TECHNIQUES

### A. Ion fractions and energy shifts in LEIS Cu scattering peaks

The measurements of ion fractions of Ne scattered from the  $\text{Cu}_3\text{Au}(100)$  surface, and shifts of the LEIS Cu scattering peak, were performed on a LEIS time-of-flight (LEIS-TOF) system, i.e., a low-energy ion scattering system, which analyzes scattered particles in the time-of-flight mode. The essential features of the system have been described previously.<sup>8</sup> The scattering chamber was maintained at a base pressure of  $3 \times 10^{-10}$  torr and at room temperature. The  $\text{Cu}_3\text{Au}$  sample, with the (100) surface exposed, was held in a manipulator which permitted both azimuthal and polar angular rotations as well as heating of the target. The laboratory scattering angle  $\Theta_L$ , was  $90.5^\circ$  and the angular acceptance of the detector was  $1.5^\circ$ . The sample had been polished by fine abrasives and a gentle electrolytic etch before mounting in the chamber. It was further cleaned by  $\text{Ar}^+$  bombardment, followed by annealing at temperatures above and then below the order-disorder critical temperature of  $390^\circ\text{C}$ . This procedure had been found to produce a well-ordered

equilibrium surface having a first layer of 50-50 Cu-Au, and a second layer of pure Cu.<sup>9,10</sup> In the limit of perfect order, the first layer of the (100) surface is comprised of pure Cu[100] rows alternating with pure Au[100] rows. LEIS spectra for the first layer, Fig. 1, were taken with the scattering plane parallel to these [100] rows, and the beam incident at  $\psi=45^\circ$  (see Fig. 1 inset). This orientation provides both channeling and blocking to suppress scattering from deeper layers. In order to scatter from the second layer, as well as the first, while shadowing deeper layers, the scattering plane was aligned with a [110] azimuth, and the beam was incident at  $\psi=35^\circ$ . Spectra were taken at a series of incident energies  $E_0$  between 2.4 and 10 keV. At each  $E_0$ , several sets of spectra were obtained, each set containing a spectrum of ions plus neutrals, and one of neutrals only, collected concurrently by deflecting ions out of the scattered beam for one second of a two-second cycle, repeated 60 to 90 times. The detector at the end of the 95-cm flight path was a 20-stage mesh electron multiplier with Cu-Be dynodes. At each  $E_0$ , spectra were typically taken from the first layer, and then from the first and second layers. Measurements were carried out over a period of several weeks, during which the sample surface was re-cleaned and reannealed periodically. In addition to the neutralization information, the Ne scattering spectra also exhibited rather surprising energy shifts in the Cu scattering peaks, which will be discussed below.

### B. Auger electrons from scattered Ne

In separate measurements in another UHV chamber, the cylindrical mirror analyzer (CMA) of a Physical Electronics model 600 scanning Auger microprobe was used to detect the Auger electrons from scattered Ne ions. In normal operation an electron gun, concentric with the CMA, provided a focused beam of electrons used to excite Auger transitions in the target material. This common method of Auger analysis was used to check the surface cleanliness of all targets used in this study. The system also contained a sputter ion gun (model 04-303) used in depth-profiling studies. With the concentric electron gun turned off, and the CMA turned on, the target surface could be bombarded with a focused beam of Ne ions in the energy range 0.25 to 5 keV. The ions were incident approximately  $40^\circ$  from the surface normal. The CMA, with an acceptance angle of  $42.5^\circ$ , could collect Auger electrons from excited Ne which had scattered through laboratory scattering angles  $\Theta_L$ , ranging from  $63.5^\circ$  to  $106.5^\circ$  (see Fig. 6 inset).

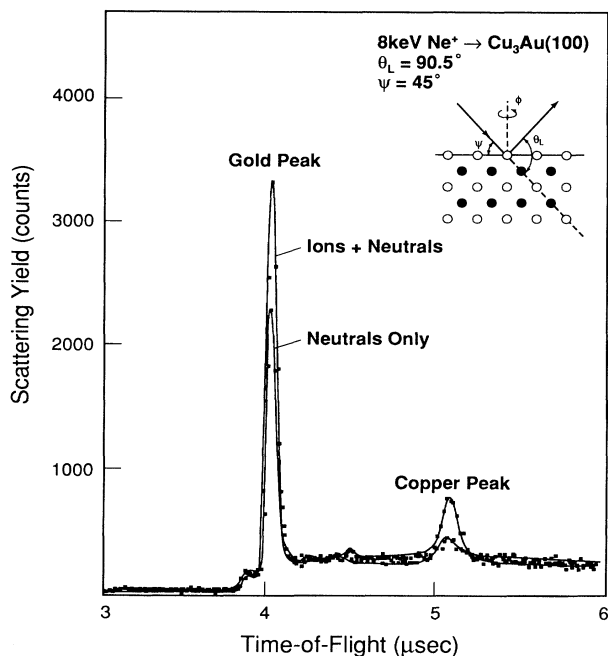


FIG. 1. Typical first-layer LEIS-TOF scattering spectra, showing a spectrum of ions plus neutrals, and the corresponding spectrum of neutrals only. The figure inset defines the azimuthal  $\phi$ , polar  $\psi$ , and laboratory-scattering  $\Theta_L$  angles. The azimuthal angle  $\phi$  for this spectrum has been set to place the scattering plane along the [100] surface row.

## III. EXPERIMENTAL RESULTS

### A. Ion fractions

The ion fraction of scattered Ne, defined by  $Y^+/Y = Y^+ / (Y^0 + Y^+)$ , the yield of ions divided by the yield of ions plus neutrals, was obtained by summing the single scattering peaks above a background line determined by points on either side of the base of the single scattering peak.<sup>10</sup> We will be referring to "single scatter-

ing” although departures from the single scattering were present in second-layer scattering. In earlier work,<sup>10</sup> computer simulation of such first-layer spectra had shown no significant contributions to the Cu or Au peaks from any scattering trajectory other than first-layer single scattering.

The curves of  $Y^+/Y$  versus  $E_0$  in Figs. 2 (first layer only) and 3 (first and second layers) show several interesting features. The curves for Ne scattered from Cu reveal a very pronounced step starting at about 4 keV, which is not present for Ne scattered from Au. The lower end of the Cu curve, below 4 keV, lies above the Au curve for first-layer scattering, but below the Au curve when second-layer scattering is included. The Au curve is lowered only slightly when second-layer scattering is included. The step in the Cu curve is present for both first layer and first- and second-layer scattering.

At low  $E_0$ , the higher ion fraction for Ne scattered from Cu, as compared to Ne scattered from Au, is associated with a lower “critical velocity”,  $v_c$  for the Ne-Cu collisions. The Au curve and the lower end of the Cu curve exhibit a trend of ion fraction with incident and scattered velocity ( $v_i, v_f$ ) predicted by the expression<sup>11,12</sup>

$$\frac{Y^+}{Y} = \exp \left[ -v_c \left( \frac{1}{v_i \sin(\psi)} + \frac{1}{v_f \sin(\theta_L - \psi)} \right) \right]. \quad (1)$$

This is based on the classic work of Hagstrum<sup>13</sup> and takes into account neutralization by electrons from the solid by both Auger and resonance transitions. The slope of natural logarithm of the ion fraction  $\log(Y^+/Y)$  versus

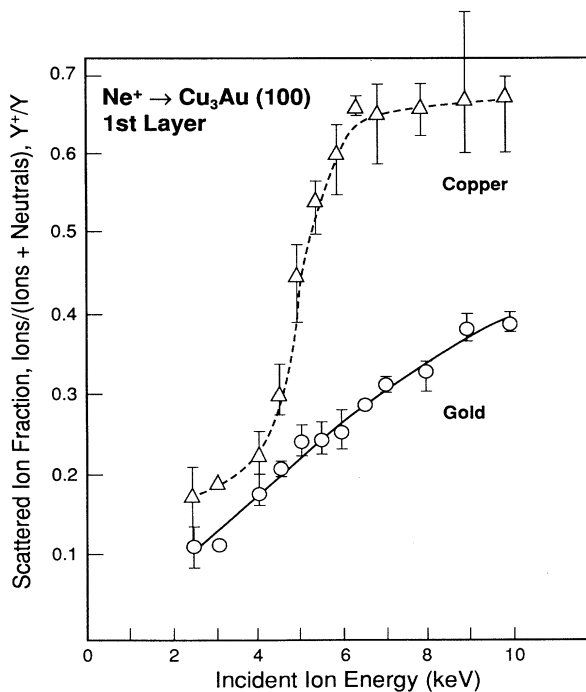


FIG. 2. Ion fractions of Ne scattered from first-layer Cu and Au atoms as a function of incident-ion energy. The plotting symbols are centered on mean values; maximum and minimum values are indicated by bars.

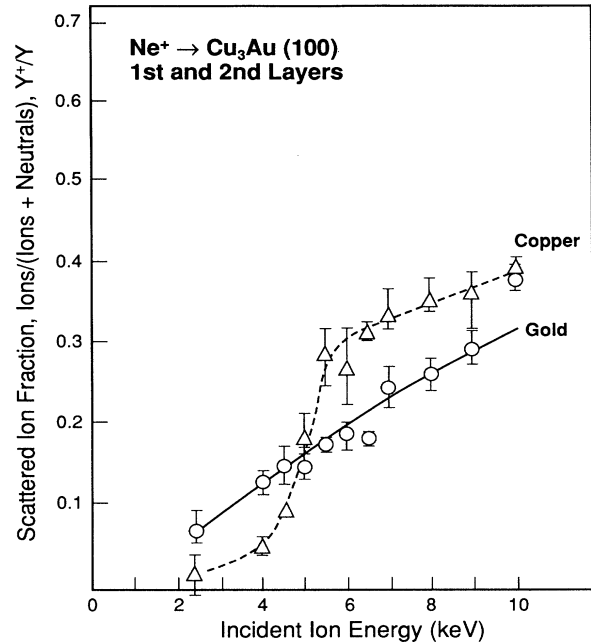


FIG. 3. Ion fractions of Ne scattering from first and second layers as a function of incident-ion energy.

$[1/(v_i \sin(\psi)) + 1/(v_f \sin(\theta_L - \psi))]$ , shown in Fig. 4 for Ne scattered from Au indicates  $v_c(\text{Au}) = 1.36 \times 10^7$  cm/sec.

When performing a composition analysis of a Cu-Au surface with 2 to 3 keV  $\text{Ne}^+$ , using an electrostatic analyzer, one would evidently need to multiply the Cu scattering yield by a correction factor of  $\sim 0.67$  due to

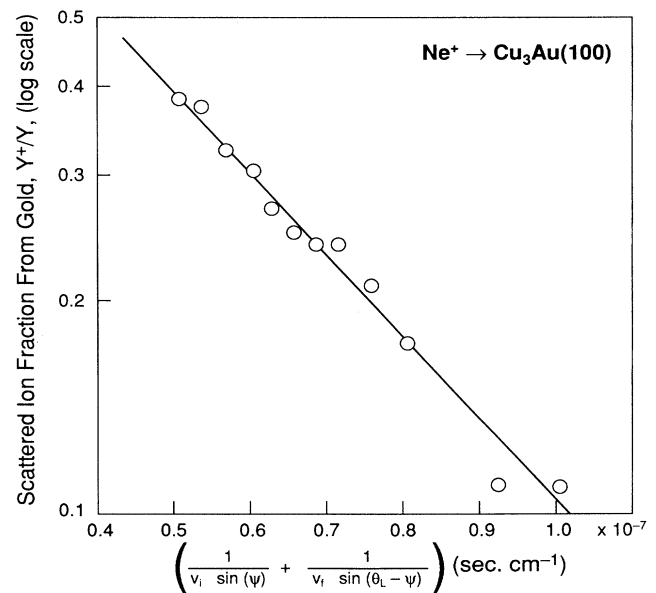


FIG. 4. Ion fractions of Ne scattered from Au in the first layer as a function of the reciprocal of the normal components of the incident and final velocities. The ordinate is plotted on a ln scale. The slope of this line gives the critical velocity  $v_c$  for Ne ion neutralization. See Eq. (1).

differences in neutralization in this low-energy range and varying smaller factors at higher energies as dictated by the ion-fraction curve. When scattering from the nearly pure Cu second layer is included (Fig. 3), the low-energy end of the Cu curve is now lower than the Au curve. This is because now two-thirds of the Cu observed is in the second layer where neutralization is more efficient, owing to higher electron densities and to a greater time spent by the ion near the surface. Computer simulations of this second-layer scattering by Buck, Wheatley, and Jackson<sup>10</sup> have shown a significant contribution to the Cu “single-scattering” peak from zig-zag scattering in the [110] surface semichannel, and these trajectories are presumably associated with high neutralization efficiency.

It is important to note that the large steps in the ion-fraction curves for Cu at  $\sim 4$  keV did not influence the total scattering yield through changes in the detector efficiency. A plot of  $Y/\sigma$  versus  $E_0$ , with an appropriate differential scattering cross section  $\sigma$  calculated for each  $E_0$  did not exhibit a corresponding step in the Cu curve.<sup>10</sup> The Cu and Au lines both had the same constant upward slope with  $E_0$  and lay close together. The slope in  $Y/\sigma$  versus  $E_0$  for both Cu and Au was attributed to a dependence of detector efficiency on particle energy. The absence of a step in the line for Cu corresponding to the step in the ion-fraction curve for Cu is evidence that the detector was equally sensitive to  $\text{Ne}^+$  and  $\text{Ne}^0$ , i.e., potential emission of electrons from the first Cu-Be dynode of the 20-stage mesh multiplier detector was much less efficient than kinetic emission.<sup>14</sup>

### B. Energy shifts in LEIS Cu scattering peaks

In extracting the ion-fraction information from the spectra we found that Cu peaks for the higher incident energies appeared at scattered energies  $E_1$ , significantly lower than predicted for elastic scattering by the kinematic equation

$$E_1 = E_0 \left[ \frac{m_1^2}{(m_1 + m_2)^2} \right] \left[ \cos\Theta_L + \left[ \frac{m_2^2}{m_1^2} - \sin^2\Theta_L \right]^{1/2} \right]^2, \quad (2)$$

where  $m_1$  is the mass of the ion,  $m_2$  is the mass of the target atom, and  $\Theta_L$  is the laboratory scattering angle. Smaller shifts of this type have been reported for Ne scattering from Mg,<sup>15</sup> and evidence of such shifts may also be seen in comparisons of experimental spectra with computer simulations of 5- and 9.5-keV Ne scattered from Cu (Ref. 10) and Ni.<sup>16</sup>

In Fig. 5 we show the energy displacements of the Cu peak relative to its position predicted for elastic scattering, assuming that the Au peak was at its predicted energy for elastic scattering. This assumption was necessary since in the LEIS-TOF system used the time scale had no independently established zero such as might be provided by light pulses produced by ions backscattering from target atoms.<sup>15</sup> We believe the assumption is justified for two reasons: There is no step in the Ne-Au ion-fraction curve, and no Auger electron emission from Ne scattered from Au atoms was observed. Souda *et al.*<sup>17</sup> have re-

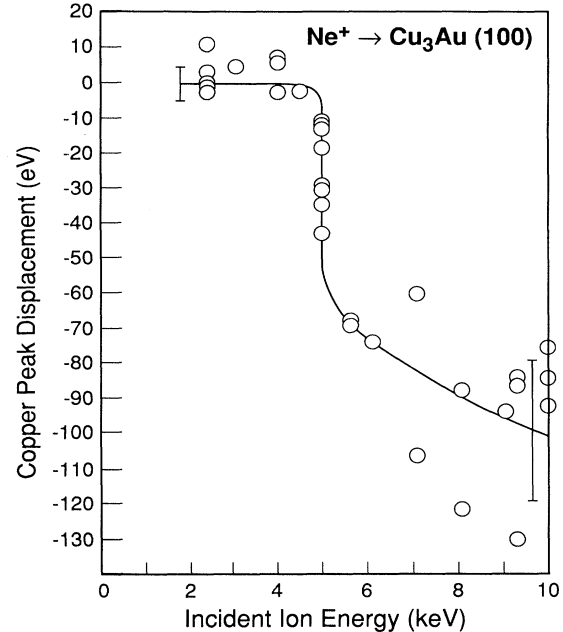


FIG. 5. Measured energy displacement of the LEIS Cu scattering peak from the energy predicted for ideal elastic scattering. If inelastic electron effects were not present in Ne-Cu scattering, the energy displacement would be zero for all incident energies.

ported at 1:10 ratio of the yield of  $\text{Ne}^+$  obtained with  $\text{Ne}^0$  incidence to that obtained with  $\text{Ne}^+$  incidence on Au for 2-keV incident energy and  $\Theta_L = 120^\circ$ . The ratio increased linearly from 0% at 600 eV, to 10% (1:10) at 2 keV. They attributed this to reionization in the Barat-Lichten model,<sup>18</sup> while also reporting much greater ratios, 50% and 70%, for Ne scattering from Sn and Ba, respectively. In the latter cases there were steps in the ion-fraction curves. This 10% ratio for Au would correspond to a 1% ion fraction at 2 keV, i.e., only a small contribution to the Au behavior shown in Figs. 2 and 4 which seems to fit the model represented by Eq. (1). Any difference in stopping-power losses for Ne in Au and Cu should be inconsequential in this case of first-layer scattering.

Figure 5 shows the energy-loss values plotted versus  $E_0$  over the same range as the ion-fraction values; a downward step occurs between 4 and 5 keV, similar to the upward step in  $Y^+/Y$  versus  $E_0$  of Figs. 2 and 3. Energy losses as high as 130 eV were observed. Scatter in the data is greater at higher energies because constant channel widths on the time axis of an LEIS-TOF spectrum correspond to larger energy increments at higher  $E_0$ , as indicated by the error bars of Fig. 5. The Cu peaks were relatively broad, owing to a high natural isotope content for Cu, so that there was some uncertainty in the selection of the channel corresponding to the scattering peak maximum. Nevertheless, the measurements were repeated on different occasions, in each case showing the same energy losses. It is interesting to note that unusually large energy losses of about 150 eV have been observed in

gas-phase, head-on  $\text{He}^+ \rightarrow \text{Ne}$  collisions leading to  $\text{Ne}^+$ .<sup>19</sup>

### C. Autoionization of scattered Ne

Electron-stimulated Auger electron spectroscopy (AES), performed on a pure Cu target before ion bombardment, showed only Auger peaks attributable to Cu, as would be expected. At this point, the CMA was calibrated to the Cu Auger doublet at 59 eV.<sup>20</sup> Ion-stimulated AES did not show these Cu Auger peaks; however, it did reveal three new peaks. These are shown in Fig. 6, after an exponential subtraction of the secondary-electron "background." The energies of these new peaks are 23.4, 26.7, and 28.8 eV. These energies are unexpected for Cu, but have been observed in various experiments on Ne gas,<sup>21–24</sup> and have been theoretically predicted for Ne.<sup>25</sup> Furthermore, this effect has previously been seen with Ne ions impacting Al (Refs. 26–28) and Mg (Ref. 15) targets. The energy resolution of the CMA used was 0.3% of the detected energy, and all spectra in a series were taken at a constant ion dose, typically 1 mC. Increasing the ion dose did not change the general peak shape or peak position.

It could be possible that the Ne Auger peaks observed were not from scattered Ne, but due to ion-stimulated AES from Ne embedded in the Cu target. However, electron-stimulated AES in the region of ion bombardment failed to show any sign of Ne Auger electrons, even under very close examination. From this it was concluded that the Ne Auger electrons measured were a product of the autoionization of scattered Ne ions, neutralized but left in an excited state as a consequence of impact with the Cu target. Furthermore, the Ne Auger peaks were not changed by sputter damage to the target.

A substantial increase in the number of Ne Auger elec-

trons detected was found in the vicinity of 4- to 5-keV incident ion energy, as shown in Fig. 7. This energy is coincident with the energy range where the ion fraction of scattered Ne increases, and  $E_1/E_0$  of Ne scattered from Cu decreases. This affirms that these three phenomena are parts of the same atomic-relaxation process.

When the same experiment was performed on pure Au targets, no Ne Auger electrons were detected, only a broad secondary-electron background. When the target material was a  $\text{Cu}_3\text{Au}(100)$  surface, Ne Auger electrons were once again detected. This indicates that the Ne autoionization process is a function of Ne-Cu collisions, and not of Ne-Au collisions. The Ne Auger peaks measured from the  $\text{Cu}_3\text{Au}(110)$  target were shifted in energy by +0.15 eV compared to those taken on the pure Cu target.

As mentioned previously, Ne Auger electrons, produced by  $\text{Ne}^+$  impact, have already been measured on other target materials. A prior study<sup>15</sup> found two Ne Auger peaks from a Mg target in the range 19 to 23 eV stimulated by Ne ions with an incident energy of 2 keV. Using Ne ions in the range 0.25 to 5 keV the present experiments were also able to detect two Auger peaks in the same energy range. Prior experiments on Al had also shown two Ne Auger electron peaks in the energy range 20 to 25 eV stimulated with incident Ne ions both in the 0.3- to 3-keV energy range<sup>26</sup> and in the 1- to 5-keV range.<sup>27,28</sup> These experiments were also repeated in the present work and were found to be in agreement with that earlier work. Further experiments on Si, Ti, and Ni showed that this phenomenon could be seen on other target materials. However, while Ne Auger electrons could be seen on low atomic number targets like Mg, Al, and Si at low incident-ion kinetic energies, heavier target materials like Ti, Ni, and Cu required higher incident-ion kinetic energies. The higher the target atomic number  $Z$  the higher the Ne ion incident energy necessary to excite

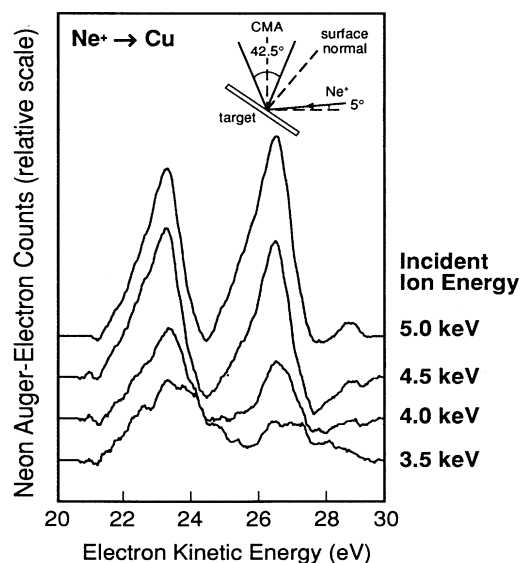


FIG. 6. Undifferentiated energy spectra of Auger electrons emitted by Ne scattered from pure Cu sample. The secondary-electron background has been removed by subtracting a fitted exponential function.

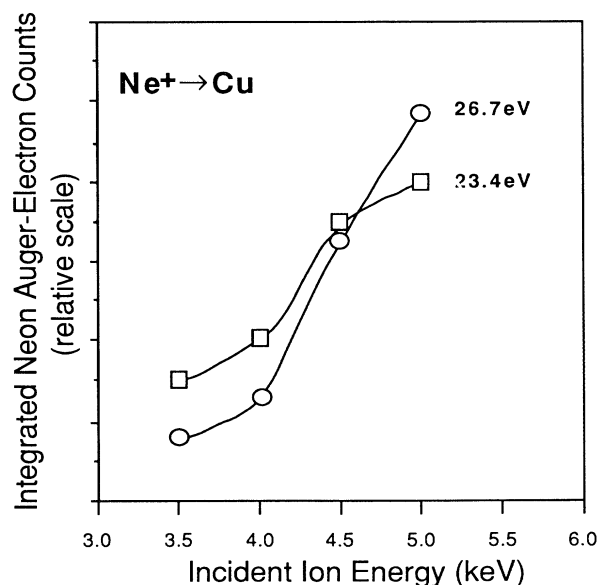


FIG. 7. Integrals of Auger peaks shown in Fig. 6.

Ne Auger transitions. This is because the distance of closest approach for a given  $E_0$  and laboratory scattering angle increases as the atomic number of the target atom increases. This would prohibit atomic-level crossings in high- $Z$  targets and thus prevent the production of Ne Auger electrons. This suggests that Ne Auger transitions might be seen on Au if the incident-ion energy were high enough. These higher ion energies were beyond the capability of the ion gun used.

#### IV. DISCUSSION

The marked increase in the ion fraction of Ne scattered from Cu, the inelastic energy loss, and the Auger emission from scattered Ne are all seen to set in as the incident energy of the  $\text{Ne}^+$  reaches 4 to 5 keV. No such behavior is observed for Ne scattered from Au. In earlier work by Luitjens *et al.* a steep increase in the ion fraction of Ne scattered from Cu setting in at 7 keV for  $\Theta_L = 30^\circ$  was reported<sup>11,12</sup> and between 2.4 and 5 keV for Ne scattered from Ni for  $\Theta_L = 90^\circ$  (Ref. 29) was also reported. However, Auger emission and inelastic energy loss were not investigated in those cases. More recently, in scattering Ne from Mg, Grizzi *et al.*<sup>15</sup> have correlated the emission of autoionization electrons, inelastic energy loss, and increase in charge state for incident energies of 1 to 4 keV. Ion fractions as large as 70% were observed, and inelastic energy losses of  $\sim 45$  eV, which were in agreement with the electronic energy required to form doubly excited  $\text{Ne}^{**}(2p^4 3s^2)$ .

The process which has been invoked to explain such behavior has been based on inner-shell hole creation in the projectile particle during the collision.<sup>11,12,15,17,18,30</sup> That is, incident ions that are neutralized on the way into the surface by resonance and Auger transitions become excited in the collision. Atomic levels of the target and projectile atoms merge into molecular orbitals (MO's). Electrons formerly in lower-energy atomic states are promoted into higher-energy MO's and, as the atoms separate, electrons in the projectile atom are left in excited atomic levels. These excited projectile atoms then decay by an Auger autoionizing process emitting energetic electrons. Due to the long lifetime of the excited state, the autoionization of the excited atoms occurs relatively far from the surface where additional neutralization is

unlikely. This causes the significant increase in the ion fraction of scattered particles.

Such a process should involve an inelastic loss in kinetic energy of the scattered particle. In the present work, Figs. 5 and 7 show that large inelastic losses did correlate with the large increases in the ion fraction of the scattered Ne and Auger electron emission from Ne. The critical energy of  $\sim 4$  keV for the onset of the reionization, Auger emission, and inelastic energy loss in these experiments corresponds to a distance of closest approach of 0.265, 0.297, or 0.292 Å as derived from the Moliere approximation to the Thomas-Fermi potential with screening radius reduced by 20%, or the same potential using the full screening radius, or the Ziegler-Biersack-Littmark potential,<sup>31</sup> respectively. These values agree with the value of 0.29 Å for a 7-keV threshold observed in  $30^\circ$  scattering of Ne from Cu by Luitjens and co-workers.<sup>11,12</sup>

To understand the reason for the larger energy losses observed here for Ne on Cu versus previous results for Ne on Mg, we resort to the diabatic MO correlation diagrams of Fig. 8, constructed following the Barat-Lichten rules.<sup>18</sup> It can be seen that in both cases, the Ne- $2p$  orbital is promoted and crosses empty (or partially empty) MO's of the same symmetry. The striking difference is in the Ne- $2s$  orbitals. In Ne-Cu it is very strongly promoted to the weakly bound Yt- $4d$  orbital. In Ne-Mg it is only slightly promoted to the Ti- $3p$  orbital. We propose that the higher-energy losses for Ne-Cu collisions signal the ionization of a  $2s$  and a  $2p$  electron leading to a  $\text{Ne}^{2+}(1s^2 2s^2 2p^3)$  state, with an excitation energy close to 100 eV. This state should decay rapidly by Auger deexcitation (AD) into  $\text{Ne}^{2+}(1s^2 2s^2 2p^4)$ , while the Ne is still close to the surface. The energy liberated in the AD process is given to a Cu outer-shell electron. This type of AD process cannot occur in free Ne because the final state  $\text{Ne}^{3+}(1s^2 2s^2 2p^3)$  is more energetic. This Auger deexcitation does not produce sharp electron peaks as those from the autoionization of  $\text{Ne}^{**}$  in vacuum. Rather, the electrons should fall into a structure approximately 7-eV wide due to the width of the conduction band of the Cu or of the  $\text{Cu}_3\text{Au}$  (Ref. 32) target. The peak would further be broadened by the fact that the short lifetime of this excited state would cause emission to occur during the collision (molecular-orbital Auger emission) where

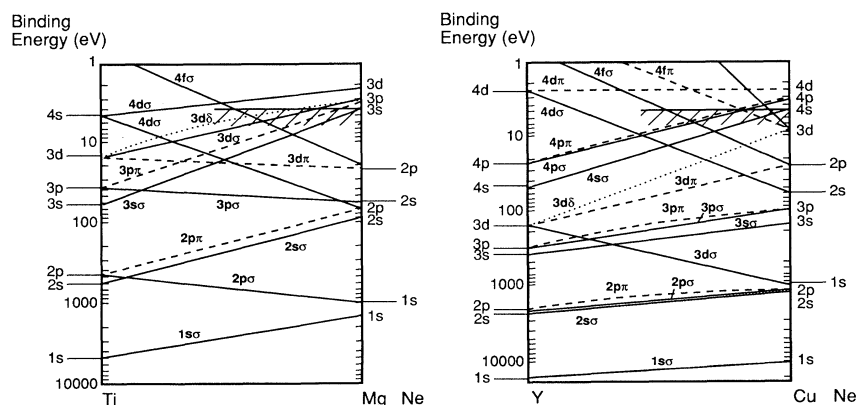


FIG. 8. One-electron diabatic molecular-orbital correlation diagrams for quasi-molecules formed transiently during Ne-Mg and Ne-Cu collisions. The crosshatched areas indicate the presence of continuum states in the valence band, for which the simplified picture of one-electron molecular states is not valid. The locations of the outer electron levels of the metals are only indicative of where they might be expected to be found within the electronic continuum.

the energy levels are changing as a function of internuclear distance. The resulting broad structure cannot be separated from the background mentioned in Sec. III C.

The picture of the inelastic Ne-Cu collision would then be as follows. When a critical  $r_c$  is reached, one or two Ne- $2p$  electrons can be excited at the crossing of the  $4f\sigma$  and the  $4s\sigma$  MO's. If two electrons are excited, the energy losses can go up to  $\sim 54$  eV  $+\varepsilon$ , corresponding to Ne( $2p^{-2}$ ) and two electrons with energy  $\varepsilon$  above the Fermi level. For slightly shorter internuclear distances,  $2s$  electrons can be excited at the crossing of the  $4d\sigma$  and  $4s\sigma$  MO's. The energy loss would be up to  $\sim 106$  eV  $+\varepsilon$ , corresponding to Ne( $2s^{-2}$ ) and two electrons with energy  $\varepsilon$  above the Fermi level. One can have different energy losses corresponding to different combinations of  $2p$  and  $2s$  vacancies and outer-shell ( $n=3,4,\dots$ ) populations, and also from excitation of Cu  $3d$  and  $4s$  electrons. The observation that the energies of the autoionization electrons do not depend on the projectile energy suggests that Ne- $2s$  vacancies are rapidly transferred to the Ne- $2p$  shell by AD involving Cu valence electrons. When the resulting Ne $^{2+}(2p^{-2})$  recedes from the surface and screening is reduced, it can capture two outer-shell electrons to the autoionizing configuration Ne $^{*+}(2p^43s^2)$ , in the manner described by Zampieri, Meier, and Baragiola.<sup>33</sup>

Finally, we consider the case of Ne-Au collisions. For such a high- $Z$  target atom, the strong electron-electron interactions do not justify the use of one-electron orbitals as those used for Cu and Mg. If we would stretch the rules to this case they would also predict the promotion of Ne- $2p$  electrons in this case. The reason why no large inelastic losses or Ne Auger lines are observed in this case is most likely related to the much stronger repulsive potential in Ne-Au collisions which do not allow for internuclear distances close enough for promotion to occur. If such is the case, one may expect to see autoionization electrons at energies higher than used in this work.

## V. CONCLUSION

The onset of an increased ion fraction for Ne scattered from Cu at 4 to 5 keV has been correlated with a decrease in the kinetic energy of the scattered Ne and the appearance of Ne Auger electrons. These three phenomena can all be attributed to inner-shell vacancy creation in the Ne during close collision with Cu. This leads to the creation of excited Ne atoms that reionize at a great distance from the solid surface by Auger autoionization. The same phenomena are not observed in Ne-Au collisions. This observation is attributed to the inability to reach sufficiently close contact for inner-shell ionization in Ne-Au collisions due to the greater repulsive potential of the Au nucleus.

## ACKNOWLEDGMENTS

The authors would like to acknowledge the financial support of the National Science Foundation, Grant No. DMR91-20668 (Materials Research Laboratory Program) (T.M.B., W.E.W., J.B.R), and Grant No. DMR91-21272 (R.A.B.), as well as the Department of Energy, Office of Basic Energy Sciences, Grant No. DE-FG03-85-13350 (R.J.G., J.G.T.). Most of the ion-scattering measurements were performed at AT&T Bell Laboratories, Murray Hill, NJ. A few were repeated on the same system after it had been moved to the University of Pennsylvania. All of the ion-induced Auger emission results were obtained at the University of Pennsylvania. We would like to thank the Surface Science Central Facility of the Penn Materials Research Laboratory for the use of the scanning Auger microprobe. The authors are grateful to G.L. Miller and Matt Soni, who provided the beam-pulsing electronics for selectable, continuously variable beam energies in the experiments performed at AT&T Bell Laboratories. We would also like to thank George Zafiridis and Greg Ford, at the University of Pennsylvania, for assistance in the data collection and data analysis, respectively.

\*Retired.

<sup>†</sup>Present address: National Institute of Standards and Technology, Gaithersburg, MD 20899.

<sup>1</sup>D. P. Smith, *J. Appl. Phys.* **38**, 340 (1967).

<sup>2</sup>R. L. Erickson and D. P. Smith, *Phys. Rev. Lett.* **34**, 297 (1975).

<sup>3</sup>A. Zartner, E. Taglauer, and W. Heiland, *Phys. Rev. Lett.* **40**, 1259 (1978).

<sup>4</sup>A. L. Boers, *Nucl. Instrum. Methods Phys. Res. B* **4**, 98 (1984).

<sup>5</sup>A. Narmann, R. Monreal, P. M. Echenique, F. Flores, W. Heiland, and S. Schubert, *Phys. Rev. Lett.* **64**, 1601 (1990).

<sup>6</sup>G. Verbist, H. H. Brongersma, and J. T. Devreese, *Nucl. Instrum. Methods Phys. Res. B* **64**, 572 (1992).

<sup>7</sup>S. R. Kasi, H. Kang, C. S. Cass, and J. W. Rabalais, *Surf. Sci. Rep.* **10**, 1 (1989); S. Valeri, *Surf. Sci. Rep.* **17**, 85 (1993).

<sup>8</sup>Y.-S. Chen, G. L. Miller, D. A. H. Robinson, G. H. Wheatley, and T. M. Buck, *Surf. Sci.* **62**, 133 (1977).

<sup>9</sup>T. M. Buck, G. H. Wheatley, and L. M. Marchut, *Phys. Rev. Lett.* **51**, 43 (1983).

<sup>10</sup>T. M. Buck, G. H. Wheatley, and D. P. Jackson, *Nucl. In-*

*strum. Meth. Phys. Res.* **218**, 257 (1983).

<sup>11</sup>S. B. Luitjens, A. J. Algra, and A. L. Boers, *Surf. Sci.* **80**, 566 (1979).

<sup>12</sup>S. B. Luitjens, A. J. Algra, E. P. Th. M. Suurmeijer, and A. L. Boers, *Surf. Sci.* **99**, 631 (1980).

<sup>13</sup>H. D. Hagstrum, *Phys. Rev.* **96**, 336 (1954).

<sup>14</sup>G. Holmen, B. Svensson, J. Schou, and P. Sigmund, *Phys. Rev. B* **20**, 2247 (1979).

<sup>15</sup>O. Grizzi, M. Shi, H. Bu, J. W. Rabalais, and R. A. Baragiola, *Phys. Rev. B* **41**, 4789 (1990).

<sup>16</sup>T. M. Buck, I. Stensgaard, G. H. Wheatley, and L. Marchut, *Nucl. Instrum. and Methods* **170**, 519 (1980).

<sup>17</sup>R. Souda, T. Aizawa, C. Oshima, S. Otani, and Y. Ishizawa, *Surf. Sci.* **194**, L119 (1988).

<sup>18</sup>M. Barat and W. Lichten, *Phys. Rev. A* **6**, 211 (1972).

<sup>19</sup>G. Gerber, A. Niehaus, and B. Steffan, *J. Phys. B* **6**, 1836 (1973).

<sup>20</sup>M. A. Hoffman, S. W. Bonner, and P. Wynblatt, *J. Vac. Sci. Technol. A* **6** (4), 2253 (1988).

<sup>21</sup>A. K. Edwards and M. E. Rudd, *Phys. Rev.* **170**, 140 (1968).

- <sup>22</sup>J. Ostgaard Olsen and N. Anderson, *J. Phys. B* **10**, 101 (1977).
- <sup>23</sup>N. Anderson and J. Ostgaard Olsen, *J. Phys. B* **10**, L719 (1977).
- <sup>24</sup>P. Bisgaard, J. Ostgaard Olsen, and N. Anderson, *J. Phys. B* **13**, 1403 (1980).
- <sup>25</sup>C. P. Bhalla, *J. Electron Spectrosc. Relat. Phenom.* **7**, 287 (1975).
- <sup>26</sup>G. E. Zampieri and R. A. Baragiola, *Surf. Sci.* **114**, L15 (1982).
- <sup>27</sup>J. Ferrante and S. V. Pepper, *Surf. Sci.* **57**, 420 (1976); S. V. Pepper and J. Ferrante, *ibid.* **88**, L1 (1979).
- <sup>28</sup>S. V. Pepper and P. R. Aron, *Surf. Sci.* **169**, 14 (1986); S. V. Pepper, *ibid.* **169**, 36 (1986).
- <sup>29</sup>T. M. Buck, G. H. Wheatley, and L. K. Verheij, *Surf. Sci.* **90**, 635 (1979).
- <sup>30</sup>E. W. Thomas, *Prog. Surf. Sci.* **10**, 383 (1980).
- <sup>31</sup>J. F. Ziegler, J. P. Biersack, and U. Littmark, *The Stopping and Range of Ions in Solids* (Pergamon, New York, 1985).
- <sup>32</sup>S. Krummacher, N. Sen, W. Gudat, R. Johnson, F. Grey, and J. Ghijsen, *Z. Phys. B* **75**, 235 (1989).
- <sup>33</sup>G. E. Zampieri, F. Meier, and R. A. Baragiola, *Phys. Rev. A* **29**, 116 (1974).